Available online at www.sciencedirect.com

SciVerse ScienceDirect

Physics Procedia 36 (2012) 1423 – 1428

Physics Procedia

Superconductivity Centennial Conference

Topographic changes in Ni-5at.%W substrate after annealing under conditions of buffer layer crystallization

A.C. Wulff *, O.V. Mishin, J.-C. Grivel

Materials Research Division, Risø National Laboratory for Sustainable Energy, Technical University of Denmark, DK-4000 Roskilde, Denmark

Abstract

Topographic changes have been studied in an annealed Ni-5at.%W substrate with a strong cube texture before and after additional annealing reproducing conditions of buffer layer crystallization. It was found that during this additional annealing the microstructure slightly coarsened and that the average depth of grain boundary grooves increased considerably for certain boundary types. Grooves at general high angle boundaries and Σ3 boundaries with large deviations from the ideal twin relationship were found to be more sensitive to the additional heat-treatment than grooves at low angle and true twin boundaries. Average groove widths increased for all boundary types. Despite the observed changes in the extent of grain boundary grooving, the mean surface roughness was almost identical before and after the additional annealing.

Keywords: Ni-5at.%W; annealing; topography; grain boundary grooving; grain boundary misorientation

1. Introduction

Over the past decade, significant efforts have been made to increase the efficiency and quality of the coated conductors, also known as the second generation of high temperature superconductors. These conductors are fabricated using strongly textured Ni-based substrates coated with a number of ceramic buffer layers (e.g. Y_2O_3/ YSZ/CeO_2) and a superconducting $YBa_2Cu_3O_{7-\delta}$ layer. The surface roughness of

* Corresponding author
E-mail address: anwu@risoe.dtu.dk

1875-3892 doi:10.1016/j.phpro.2012.06.147

the substrate is an important parameter that should be controlled to enable good surface quality of the final superconducting tape. The mean surface roughness of the annealed substrate does not only depend on the surface roughness of the tape in the cold-rolled condition [1], but is also affected by thermal grain boundary (GB) grooving [2]. Whereas the roughness of the substrate is measured in the delivery condition, topographic changes may occur during further processing used to fabricate superconducting tapes. For example, crystallization of the buffer layers [3,4] usually involves temperatures higher than those applied for recrystallization annealing of the heavily rolled material, which can modify the surface conditions of the substrate. The aim of this work is to characterize topographic changes during annealing that reproduces the heat-treatment used for buffer layer crystallization. In the present experiment, atomic force microscopy (AFM) is combined with the electron backscatter diffraction (EBSD) technique to relate grain boundary grooving to crystallographic characteristics of grain boundaries.

2. Experimental

2.1. Material and processing

A Ni-5at.%W ingot was prepared by arc melting of 99.99% pure metals. The obtained ingot was homogenized at 1025°C for 87 hours and hot forged into a rectangular shape of 8×12×97 mm, using 0.5 mm thickness reductions per stroke. The resulting oxide formed on the surface was removed mechanically. The material was then cold-rolled using mirror-finished rolls, applying < 5% reductions per pass. The final thickness of the rolled tape was 120 μm, which corresponds to a total thickness reduction of 98 %. The tape was then recrystallized during annealing in a protective atmosphere of 5% H_2 in N_2 at 1000°C for 2 hours. Several samples were further annealed in the protective atmosphere at 1025°C for 1 hour, i.e. under conditions that are frequently used for crystallization of a ceramic buffer layer [3,4].

2.2. AFM characterization

The surface topography was investigated using both AFM and scanning electron microscopy (SEM). AFM characterization was conducted in contact mode scanning over ~17,000 μm^2 in several regions, where scans were made after annealing at 1000°C and again after annealing at 1025°C in the same regions. Non-linear artifacts due to the AFM scanner exceeding its linear scanning regime were treated using the standard data correction [5]. The arithmetic surface roughness was used in this work to characterize the mean roughness taking grain boundary grooving into account. When considering the geometry of GB grooves, the groove depth was defined as the distance from the groove root to the maxima and the groove width was measured between the maxima on either side of the groove root [6]. The depth and width of GB grooves were compared before and after the additional annealing at boundaries that did not migrate during this additional heat treatment. Analysis of GB grooves at other (migrating) boundaries that did not only create new GB grooves, but also left grooves behind in the interior of coarsened grains, will be presented elsewhere.

2.3. EBSD analysis

The EBSD technique was used for analyzing misorientations across grain boundaries and for measuring the average grain size. High angle grain boundaries (HAGBs) were defined as boundaries between grains with misorientations greater than 15°. Low angle grain boundaries (LAGBs) were defined as boundaries between grains with misorientations 1.5 – 15°. Based on a previous work on copper [7], twin boundaries were classified as Σ3 boundaries with a deviation from the ideal 60°<111>

misorientation, $\Delta\theta < 3°$. These twin boundaries could also be clearly identified in the microstructure based on their morphological features. Boundaries formed between twins and non-matrix cube-oriented neighbors [8], and satisfying Brandon's criterion [9] for the Σ3 misorientation with large ($\Delta\theta = 3$ - 8.66°) deviations from the ideal twin relationship are termed "*other* Σ3 boundaries" in this work.

3. Results

The microstructure obtained after annealing at 1000°C is characterized by a small average grain size, 25 μm (including annealing twins), and a very strong cube {001}<100> texture. Narrow annealing twins within cube-oriented grains belong to the {212}<122> component. The fraction of LAGBs identified by EBSD in this microstructure was above 80%.

An SEM image and a corresponding EBSD map from a small region are shown in Fig 1. In the EBSD map (Fig 1b), LAGBs and HAGBs are shown by gray and black lines, respectively. Red lines correspond to twin boundaries, and blue lines show *other* Σ3 boundaries with large deviations from the ideal twin relationship. The latter boundaries are formed between twins and neighboring grains slightly disoriented from the matrix grain. This situation is typically observed when grain growth occurs in a strongly textured material containing annealing twins [8,10]. Inspection of Fig 1 reveals that grooves at coherent twin boundaries (CTBs) are less prominent than grooves at any other boundary type. Whereas very little grooving was also seen at boundaries with misorientations less than 5°, grooving at other LAGBs was more significant. Deep grooves typically developed at general HAGBs, incoherent twin boundary (ITB) segments and *other* Σ3 boundaries (see Fig 1a).

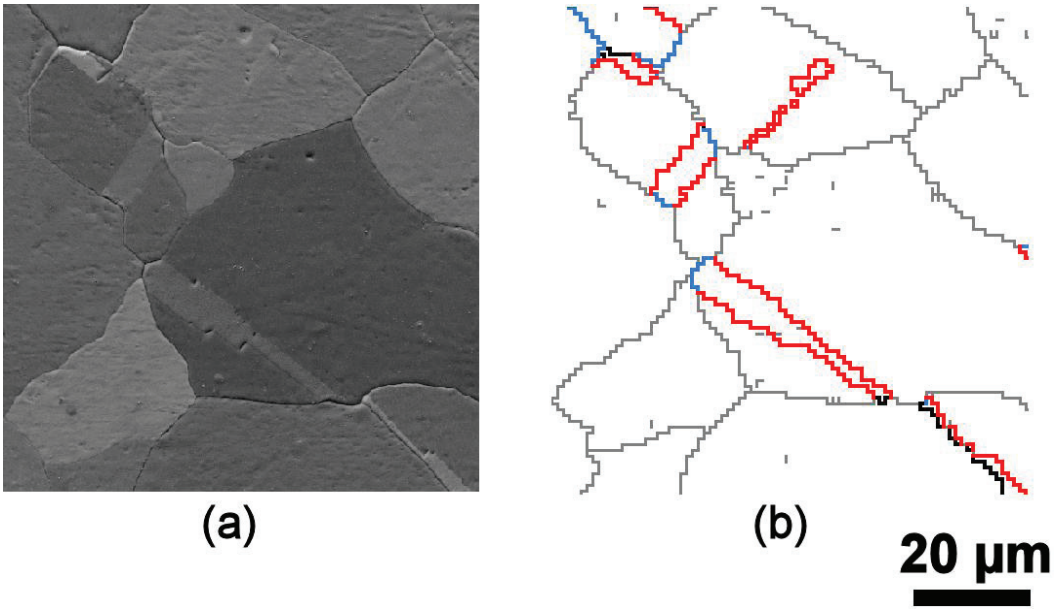

Fig. 1. Different boundary types in the microstructure annealed at 1000°C for 2 h: (a) SEM image and (b) EBSD map from the same region. In (b) low angle (1.5–15°) misorientations and general HAGBs are shown by gray and black lines, respectively. Red lines correspond to twin Σ3 boundaries ($\Delta\theta < 3°$) and blue lines show *other* Σ3 boundaries with larger deviations $\Delta\theta = 3 – 8.66°$ from the ideal twin relationship.

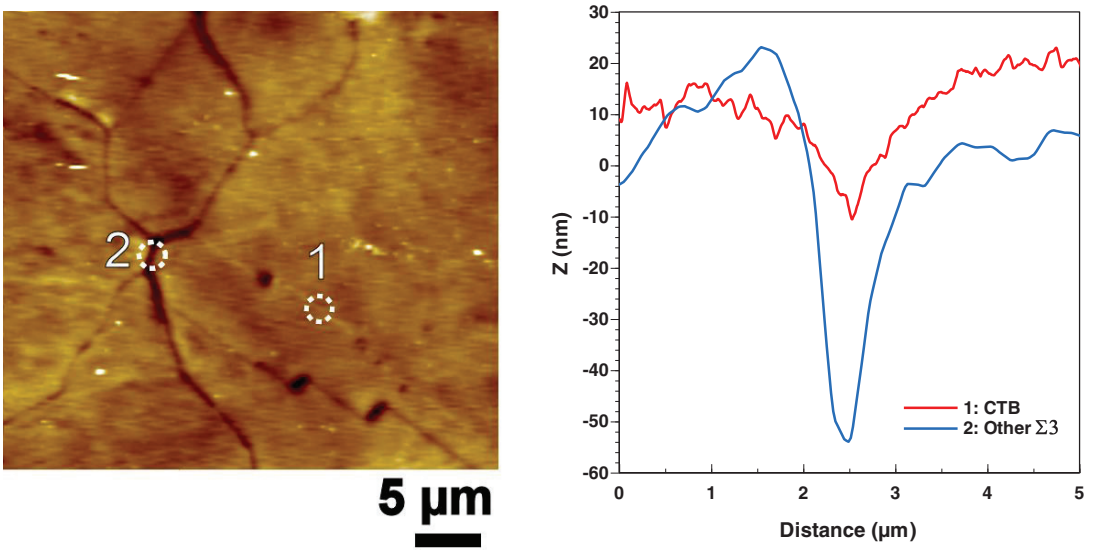

Fig. 2. AFM data for the region in Fig 1: (a) AFM micrograph where the marks "1" and "2" correspond to CTB and *other* Σ3 boundaries, respectively. (b) Profiles along line scans for these two boundaries.

An AFM micrograph from the region sampled in Fig 1 is presented in Fig 2a. To illustrate the difference between two different Σ3 boundary types, GB profiles were analyzed across boundaries marked "1" and "2" in Fig 2a. These two boundaries are classified in our work as either coherent twin or *other* Σ3 boundaries. From Fig 2b it is apparent that GB grooves at these two boundaries are very different, i.e. that the groove at the CTB is shallower than the groove at the *other* Σ3 boundary.

Average depths of grooves at 34 stationary boundaries in several regions are given in Fig 3a. It is seen that the smallest average groove depth was recorded for CTBs, followed by LAGBs. *Other* Σ3 boundaries and ITB segments demonstrated deeper grooves than the former two boundary types. Note that since ITB segments were very short, it was difficult to unambiguously determine, based on the available micrographs, whether short ITB segments were truly stationary, i.e. whether they stayed exactly in the same positions before and after the additional annealing. Therefore, parameters of grooves at ITB segments are not included in Fig 3. Considering all measured boundaries, general HAGBs were characterized by the greatest average groove depth.

Additional annealing at 1025°C resulted in a slightly larger average grain size, 29 µm, compared to that in the initial recrystallized substrate. AFM analysis of GB grooving at the same boundaries before and after the additional heat treatment indicated that the average groove depth did not significantly change for LAGBs and CTBs. However, for *other* Σ3 boundaries and especially for HAGBs the average groove depths increased considerably (see Fig 3a). The additional annealing also resulted in increased groove widths for all boundary types (Fig 3b).

The mean surface roughness of the substrate before and after additional annealing was found to be 10.7 and 10.3 nm, respectively.

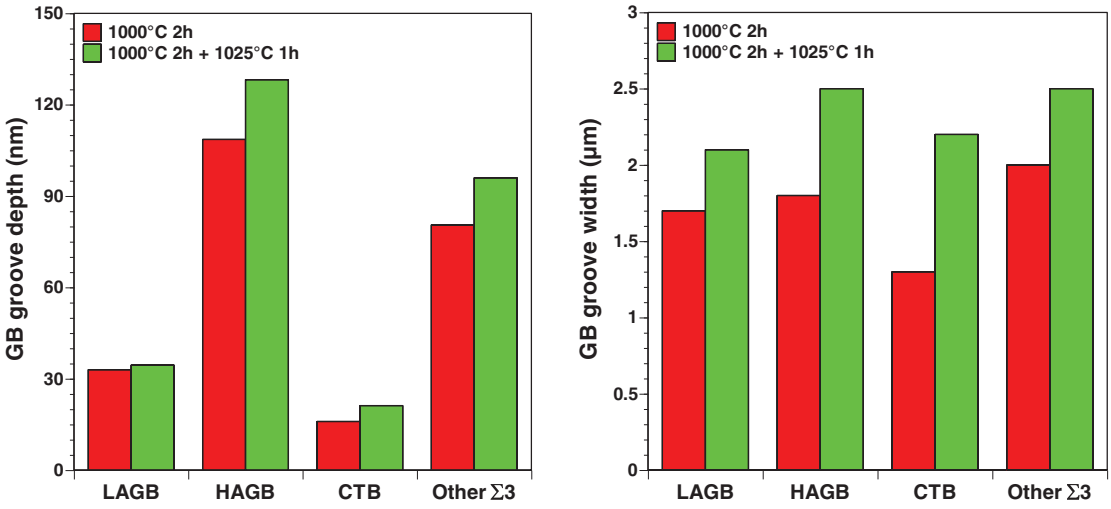

Fig. 3. Average parameters of GB groove depths (a) and widths (b) recorded from AFM data for 34 stationary boundaries before and after additional annealing.

4. Discussion

The results obtained in the present experiment demonstrate that additional heat treatment at 1025°C for 1 h alters the microstructure of the annealed Ni-5at.%W substrate. Although the additional annealing treatment was comparatively short and the temperature was only slightly higher than the temperature used for preparing the initial condition, the mean grain size has increased. Also, average depths of GB grooves at general HAGBs and *other* Σ3 boundaries increased considerably compared to those in the initial substrate (see Fig 3a). It is expected that such a substantial increase in GB grooving at these boundaries during additional annealing can be diminished either by reducing the annealing temperature below 1025°C or by decreasing the duration of annealing to < 1 h.

It is significant that in both annealed conditions HAGBs and Σ3 boundaries with large deviations for the ideal twin relationship, on average, developed deeper grooves than CTBs and LAGBs, which reflects differences in structural parameters of the different boundary types. It is therefore not surprising that a large scatter in the depth of groves at Σ3 boundaries has been obtained in several studies, where correlations between the extent of thermal grooving and GB misorientation (Σ-value) were studied [11,12]. Since boundary planes for coherent and incoherent twin boundaries are different and since other non-twin boundaries can also satisfy the generous Brandon criterion for the Σ3 misorientation, it is reasonable to distinguish between different kinds of Σ3 boundaries when linking the extent of various annealing phenomena to the boundary type.

Interestingly, despite the fact that GB grooves at general HAGBs and *other* Σ3 boundaries became much deeper after the additional annealing, no significant increase was observed for the mean surface roughness. It should be noted that the summed fraction of boundaries within the two groups that demonstrated substantially increased groove depths after annealing at 1025°C for 1 h was only 7% and, therefore, deeper grooves at these boundaries could not appreciably increase the mean surface roughness

compared to that in the initial substrate. It can be suggested that for the given heat-treatment the roughening effects due to increased grooving at certain boundaries could effectively be counterbalanced by diffusional smoothening of the surface [2].

5. Conclusions

1. Different boundary types in the annealed Ni-5at.%W substrate were grooved to a different extent. The smallest average depth was recorded for coherent twin boundaries, followed by low angle grain boundaries. Incoherent twin boundary segments and Σ3 boundaries with large deviations from the ideal 60°<111> relationship demonstrated deeper grooves than the former two boundary types. General high angle boundaries were characterized by the greatest average groove depth.

2. Additional annealing at 1025°C for 1 h slightly coarsened the microstructure. Comparison of groove parameters before and after this additional annealing at 34 stationary boundaries revealed that the average depth increased substantially for grooves at high angle boundaries and Σ3 boundaries with large deviations from the ideal twin misorientation. Changes in the average groove depth recorded for the other boundary types were less significant. Average groove widths increased for all boundary types. Despite the observed changes in the extent of grain boundary grooving, the mean surface roughness was almost identical before and after the additional annealing.

Acknowledgements

This work was supported by the Danish Ministry of Science, Technology and Innovation under contract number 09-065234. The authors gratefully acknowledge Dr. Y. Zhao and Mr. O. Trinhammer for valuable discussions of AFM measurements.

References

[1] Wulff AC, Mishin OV, Grivel J-C. *J Supercond Nov Magn* 2012; DOI: 10.1007/s10948-011-1303-5.

[2] Truchan TG, Rountree FH, Lanagan MT, McClellan SM, Miller DJ et al. *IEEE Trans Appl Supercond* 2000;**10**:1130–3.

[3] Aslanoglu Z, Akin Y, El-Kawni MI, Sigmund W, Hascicek YS. *Physica C* 2003;**384**:501–6.

[4] Zhao Y, Grivel J-C, Abrahamsen AB, Pavlopoulos D, Bednarcik J, von Zimmermann M. *IEEE Trans Appl Supercond* 2011;**21**:2912–5.

[5] Bonnell DA, Huey BD. In: Bonnell DA, editor. *Scanning Probe Microscopy and Spectroscopy*, 2nd edn, New York: Wiley; 2001, p.32–42.

[6] Mullins WW, Shewmon PG. *Acta Metall* 1959;**7**:163–70.

[7] Mishin OV, Huang X. *Mater Sci Forum* 1999;**294**–**296**:401–4.

[8] Mishin OV, *J Mater Sci* 1998;**33**:5137–43.

[9] Brandon DC, *Acta Metall* 1966;**14**:1479–84.

[10] Mishin OV, Gottstein G, *Mater Sci Eng* 1998;**A249:**71–8.

[11] Gladstone TA, Moore JC, Wilkinson AJ, Grovenor CRM. *IEEE Trans Appl Supercond* 2001;**11**:2923–6.

[12] Skidmore T, Buchert RG, Juhas MC, *Scripta mater* 2004;**50**:873–7.